Investigation of Shear Wave Propagation in Two-Dimensional Systems with Lorentzian-Correlated Disorder

M.O. Sales[a], L. D. da Silva[b], M. S. S Junior[c], F. A. B. F. de Moura[c]

[a]*IFMA Campus São João dos Patos, rua Padre Santiago, s/n, Centro, São João dos Patos-MA, 65665-000, Brazil*
[b]*Escola Estadual Professor Theotônio Vilela Brandão, R. Cel. Adauto Gomes Barbosa, s/n - Poço, Maceió-AL, 57025-045, Brazil*
[c]*Instituto de Física, Universidade Federal de Alagoas, Maceió-AL, 57072-970, Brazil*

Abstract

In this study, we investigate the propagation of shear vibrations in a rectangular system where disorder is introduced through the compressibility term, exhibiting Lorentzian spatial correlations. Our primary objective is to understand how these correlations influence the behavior and velocity of harmonic mode packets as they travel through the system. To achieve this, we employ a finite difference formalism to accurately capture the wave dynamics. Furthermore, we analyze how the spectral composition of the incident pulse affects wave propagation, shedding light on the interplay between disorder correlations and wave transport. By systematically exploring these factors, we aim to deepen our understanding of the fundamental mechanisms governing shear vibration propagation in disordered media.

1. Introduction

In wave propagation studies, acoustic systems, including shear vibrations, serve as fundamental models for investigating the complex interactions between waves and the medium they traverse.[1,2,3,4,5,6,7,8,9,10,11,12,13,14,15] While the behavior of sound waves in ordered and homogeneous media is well-understood, wave dynamics in disordered systems introduce layers of complexity that remain to be fully explored.[16] In recent years, the study of acoustic modes in disordered systems has gained attention, attracting researchers from fields such as physics, engineering, and materials science.

Disordered systems, defined by structural randomness or irregularities, offer both challenges and opportunities in the study of wave phenomena. Unlike ordered systems, where wave propagation is predictable, disordered systems display phenomena such as multiple scattering, Anderson localization, and mode

Email address: fidelis@fis.ufal.br (F. A. B. F. de Moura)

hybridization.[17,18] These effects result from the interplay between wave interference and scattering induced by disorder, leading to complex and often surprising wave behavior.[19] Understanding acoustic modes in disordered systems has important implications for various fields. In materials science, controlling acoustic wave propagation in disordered media could lead to the design of new materials with specific acoustic properties, such as enhanced sound insulation or waveguiding capabilities.[20] Disordered systems also hold promise in photonics and optoacoustics, providing platforms for robust light-matter interactions and paving the way for innovations in random lasers and optical communication.[21] Moreover, the study of acoustic modes in disordered media has practical applications in areas such as non-destructive testing, medical imaging, seismic analysis, and telecommunications.[22,23] By understanding the mechanisms behind wave propagation in these media, researchers hope to leverage their inherent complexity for technological innovations.

The behavior of elastic waves in heterogeneous media with off-diagonal disorder and long-range correlations was explored in,[24] where the authors examined how these factors influence wave dynamics. In,[25] researchers studied acoustic wave localization in one-dimensional systems with chaotic elasticity, using numerical methods to analyze localized modes. Additionally, the work in[26] investigated the propagation of acoustic waves in two-dimensional disordered media with both short- and long-range correlations. Reference[27] provides a comprehensive analysis of how correlated disorder influences localization in certain low-dimensional systems, resulting in anomalous (non-exponential) localization. The study shows that long-range correlations can suppress or modify traditional Anderson localization, significantly affecting wave transport properties.

In this work, we investigate the propagation of shear vibrations in disordered systems, with a particular focus on a rectangular geometry where disorder is introduced through the compressibility term. Specifically, we consider a system in which the disorder exhibits Lorentzian spatial correlations, allowing us to explore the impact of strong correlations on wave propagation. To achieve this, we analyze the behavior of harmonic mode packets as they travel through the system, employing a finite difference scheme to ensure accurate numerical modeling of the wave dynamics. A key aspect of our study is to determine how the presence of correlated disorder affects the dispersion and velocity of shear modes. Additionally, we examine the influence of the spectral composition of the incoming wave packet, investigating how different frequency components interact with the disordered medium. By systematically varying the characteristics of both the disorder and the excitation, we aim to gain insights into the mechanisms governing shear wave transport in disordered environments.

2. Model

The propagation of shear vibrations in a two-dimensional disordered medium of size $L \times N$ with uniform mass density at position $\vec{r}$ can be described by the scalar wave equation,[26,28] which governs the displacement field $\psi(\vec{r}, t)$ in an

elastic medium:

$$\frac{\partial^2 \psi(\vec{r},t)}{\partial t^2} = \vec{\nabla} \cdot [\Pi(\vec{r})\vec{\nabla}\psi(\vec{r},t)], \tag{1}$$

where $\psi(\vec{r},t)$ represents the displacement field at position $\vec{r}$ and time t. This scalar quantity describes the transverse displacement of the medium due to shear vibrations, and it indicates how much each point of the material moves in the direction perpendicular to the plane of propagation. In the case of shear vibrations, $\psi(\vec{r},t)$ can be thought of as the amplitude of the deformation at any point in space and time. The units of ψ are typically units of length. On the other hand, $\Pi(\vec{r})$ represents the bulk stiffness or elastic modulus at position $\vec{r}$. It characterizes the resistance of the medium to deformation at a given point, and it governs how the medium's internal forces respond to the strain induced by the displacement $\psi(\vec{r},t)$. $\Pi(\vec{r})$ can vary spatially, reflecting heterogeneities in the material's properties, such as varying stiffness or elasticity across the medium. In a homogeneous material, $\Pi(\vec{r})$ would be a constant value, typically the Young's modulus E for a linear elastic material, but it can be position-dependent in a disordered system. The units of $\Pi(\vec{r})$ are characteristic of force per unit length or pressure per unit area. We assume a constant mass density of 1, independent of $\vec{r}$. This simplifies the model by normalizing the mass density in dimensionless units, ensuring consistency with the chosen scale of the problem.In this equation, the characteristic unit of time is given by $\zeta/\sqrt{\langle\Pi\rangle}$, where ζ represents a relevant length scale (such as the lattice spacing in a discretized version of the system), and $\langle\Pi\rangle$ is the average elastic modulus. This implies that time is measured in units of the propagation time across a characteristic length, which is determined by the medium's stiffness. This equation describes how mechanical perturbations evolve in time under the influence of spatially varying stiffness, a characteristic of disordered elastic systems. The right-hand side accounts for the inhomogeneous mechanical response due to spatial fluctuations in $\Pi(\vec{r})$. To better understand the structure of Eq. (1), we expand the term inside the divergence:

$$\begin{aligned} \vec{\nabla} \cdot [\Pi(\vec{r})\vec{\nabla}\psi(\vec{r},t)] &= \partial_x \Pi(\vec{r})\partial_x \psi(\vec{r},t) + \partial_y \Pi(\vec{r})\partial_y \psi(\vec{r},t) \\ &+ \Pi(\vec{r})[\partial_x^2 \psi(\vec{r},t) + \partial_y^2 \psi(\vec{r},t)]. \end{aligned} \tag{2}$$

This expansion explicitly shows that the wave propagation is affected both by gradients of the stiffness field (first two terms) and by the local Laplacian of the displacement field (last term). The presence of $\Pi(\vec{r})$ outside the Laplacian term distinguishes this equation from the standard wave equation in homogeneous media. The derivation of Eq. (1) follows from the fundamental principles of wave motion in elastic continua, as discussed in Symon (1960, Mechanics, 2nd ed.), particularly in Chapters 8-1 to 8-5.[29] In this reference, the equation governing small oscillations in a nonuniform elastic medium is derived step by step, providing a rigorous foundation for our model. A similar formulation has also been applied in disordered lattice models.[26] To numerically solve the wave equation in two dimensions, we apply the finite difference method on a rectangular grid. The displacement function $\psi(\vec{r},t)$ is discretized as $\psi_{i,j}^n$, where the indices

i, j correspond to the spatial positions $x = i\delta x$ and $y = j\delta y$, while n denotes the time steps $t = n\delta t$. The medium's compressibility $\Pi(\vec{r})$ is discretized as $\Pi_{i,j}$. To ensure numerical stability, we adopt spatial discretization steps $\delta x = \delta y = 1$, which define the typical lattice spacing in dimensionless units and correspond to the characteristic length scale ζ previously introduced to describe the propagation time scale. A sufficiently small time step of $\delta t \approx 10^{-3}$ is employed to guarantee the accuracy and stability of the numerical integration. The second-order time derivative is approximated using a central difference scheme:[26,30,31,32]

$$\frac{\partial^2 \psi(\vec{r}, t)}{\partial t^2} \approx \frac{\psi_{i,j}^{n+1} - 2\psi_{i,j}^{n} + \psi_{i,j}^{n-1}}{\delta t^2}. \tag{3}$$

The spatial derivatives are approximated using higher-order finite difference schemes to improve accuracy and reduce numerical dispersion:

$$\partial_x^2 \psi(\vec{r}, t) \approx \frac{-\psi_{i+2,j}^{n} + 16\psi_{i+1,j}^{n} - 30\psi_{i,j}^{n} + 16\psi_{i-1,j}^{n} - \psi_{i-2,j}^{n}}{12(\delta x)^2}, \tag{4}$$

$$\partial_x \psi(\vec{r}, t) \approx \frac{-\psi_{i+2,j}^{n} + 8\psi_{i+1,j}^{n} - 8\psi_{i-1,j}^{n} + \psi_{i-2,j}^{n}}{12\delta x}. \tag{5}$$

Similarly, for the y-direction:

$$\partial_y^2 \psi(\vec{r}, t) \approx \frac{-\psi_{i,j+2}^{n} + 16\psi_{i,j+1}^{n} - 30\psi_{i,j}^{n} + 16\psi_{i,j-1}^{n} - \psi_{i,j-2}^{n}}{12(\delta y)^2}, \tag{6}$$

$$\partial_y \psi(\vec{r}, t) \approx \frac{-\psi_{i,j+2}^{n} + 8\psi_{i,j+1}^{n} - 8\psi_{i,j-1}^{n} + \psi_{i,j-2}^{n}}{12\delta y}. \tag{7}$$

The derivatives of $\Pi(\vec{r})$ are approximated as:

$$\partial_x \Pi(\vec{r}) \approx \frac{-\Pi_{i+2,j} + 8\Pi_{i+1,j} - 8\Pi_{i-1,j} + \Pi_{i-2,j}}{12\delta x}, \tag{8}$$

$$\partial_y \Pi(\vec{r}) \approx \frac{-\Pi_{i,j+2} + 8\Pi_{i,j+1} - 8\Pi_{i,j-1} + \Pi_{i,j-2}}{12\delta y}. \tag{9}$$

By substituting these approximations into the wave equation, we obtain the recurrence relation:

$$\psi_{i,j}^{n+1} = 2\psi_{i,j}^{n} - \psi_{i,j}^{n-1} + \delta t^2 \left(\sum_{z=x,y} \left[\partial_z \Pi \cdot \partial_z \psi + \Pi \left(\partial_x^2 \psi + \partial_y^2 \psi \right) \right] \right). \tag{10}$$

This recurrence relation is used in numerical algorithms to iteratively compute wave propagation in disordered media. The finite difference method is widely applied in fields such as acoustics, geophysics, and elasticity.[33,34,35,36,37] The choice of this formalism is justified by several factors, making it an efficient and effective approach for this particular problem. The explicit time-stepping scheme used in our approach is not computationally expensive and is well-suited

for simulations. Furthermore, this method naturally fits structured Cartesian grids, which helps reduce computational complexity when compared to unstructured mesh-based methods like the finite element method (FEM),[38] typically preferred for irregular geometries. The use of high-order finite difference stencils, such as the fourth-order central difference approximations employed in our formulation, improves the accuracy of spatial derivatives, minimizing numerical dispersion and ensuring precise wave propagation. *The time step $\delta t \approx 10^{-3}$ was chosen based on numerical stability considerations. Tests with smaller values (e.g., $\delta t = 5 \times 10^{-4}$ and 10^{-4}) showed no significant differences in the results, confirming that the chosen value ensures stability without incurring unnecessary computational cost.*

In this study, the bulk compressibility $\Pi_{i,j}$ is modeled as a disordered distribution exhibiting Lorentzian correlations. These correlations describe the interaction between spatial points, decaying slowly as the distance between them increases. To generate this disordered landscape, we first compute the two-dimensional (2D) distribution $B_{i,j}$, defined as:

$$B_{i,j} = \sum_{o,p} \frac{1}{1 + \left(\frac{\sqrt{(i-o)^2 + (j-p)^2}}{\Lambda} \right)^2} \zeta_{o,p}, \tag{11}$$

where $\zeta_{o,p}$ represents a random field consisting of $L \times N$ uniformly distributed random values in the interval $[-1, 1]$. The term Λ represents the correlation length, which determines how far the Lorentzian correlations extend within the system. It measures the distance over which correlations remain significant. The unit of Λ is distance (for example, the lattice spacing), and it quantifies the spatial range of the correlations. The Lorentzian factor $\frac{1}{1+(r/\Lambda)^2}$, where $r = \sqrt{(i-o)^2 + (j-p)^2}$ represents the Euclidean distance between points (i, j) and (o, p), acts as a spatial filter. This filter ensures that the influence of distant points decays smoothly, with the decay rate controlled by Λ. In the summation above, the term corresponding to $r = 0$ (i.e., $i = o$ and $j = p$) should not be considered. As the distance r increases beyond Λ, the contribution of distant points to the sum diminishes rapidly, highlighting the importance of nearby sites in determining the value of $B_{i,j}$. When $\Lambda \ll L$, the correlations are weak (extremely short-range). In this regime, the influence of distant points is negligible, and the system roughly behaves as if it contains an uncorrelated disorder distribution. On the other hand, when Λ is comparable to L, the system exhibits strong correlations, with distant points still showing significant statistical dependence. The case $\Lambda = 0$, assuming $r > 0$, corresponds to the pure system—one without disorder. In this case, it becomes meaningless to talk about correlated disorder; therefore, it is an undesirable limit of this formula. In summary, Λ represents the characteristic length over which correlations are significant. Small values of Λ correspond to weak correlations, meaning that Λ is small but not zero, while values of Λ on the order of the system size correspond to strong correlations.

In practical computations, the summation over indices o and p can be lim-

ited to points within a finite radius around (i, j) because the Lorentzian function quickly decays. For instance, when $|i - o|$ and $|j - p|$ exceed a threshold of approximately 150 lattice sites, the influence of terms in the summation becomes negligible. Thus, the summation is efficiently truncated, with only local neighborhoods of size $|i - o| < 150$ and $|j - p| < 150$ being considered for each $B_{i,j}$ value. This truncation greatly reduces computational overhead without significantly affecting the accuracy, especially when the correlation length Λ is smaller than or on the order of 100. For small values of Λ, the disorder distribution becomes rougher, while for larger values of Λ, the correlations persist over longer distances, resulting in a smoother disorder profile. After constructing the 2D field $B_{i,j}$, it is necessary to normalize it so that the disorder has desirable statistical properties. Specifically, we normalize the field such that the mean value $\langle B_{i,j} \rangle = \sum_{i,j} B_{i,j}/(LN)$, representing the average value of the field at position (i, j), is zero, and the term $\langle B_{i,j}^2 \rangle = \sum_{i,j} B_{i,j}^2/(LN)$, representing the average second moment of the field, is normalized to unity. This ensures that the disorder distribution is centered around zero, with fluctuations that are statistically well-defined and bounded. Once the normalized distribution $B_{i,j}$ is obtained, the bulk compressibility at each point (i, j) is determined through the following relation: $\Pi_{i,j} = \tanh(B_{i,j}) + 2.$. This transformation ensures that the compressibility values remain physically meaningful. The hyperbolic tangent function compresses the values of $B_{i,j}$, preventing $\Pi_{i,j}$ from becoming excessively large, while the constant shift of $+2$ guarantees that the compressibility remains strictly positive, avoiding any unphysical negative values. Moreover, this method retains the inherent Lorentzian correlations in the original $B_{i,j}$ field, ensuring that the bulk compressibility $\Pi_{i,j}$ mirrors the desired spatial structure of the disorder. This process thus allows for the generation of a well-behaved, Lorentzian-correlated disordered medium where the compressibility $\Pi_{i,j}$ exhibits controlled spatial variations.

Our investigation focuses on analyzing the propagation characteristics of pulses in a system described by a specific mathematical framework. In particular, we performed a series of numerical simulations to study how these pulses travel through a rectangular lattice structure, which serves as a model for various physical systems. The left boundary of the lattice is connected to an oscillator that plays a crucial role in injecting pulses into the system. These pulses are mathematically represented by the expression

$$\psi_{i,j=0}(t) = \exp\left[-\frac{t^2}{\sigma_T}\right] \cos(\omega t), \tag{12}$$

where ω denotes the frequency of the pulse (in units of $\sqrt{< \Pi >}$) and σ_T controls the temporal width of the pulse envelope. The Gaussian factor $\exp\left[-\frac{t^2}{\sigma_T}\right]$ ensures that the pulse is localized in time, while the cosine component introduces oscillatory behavior, making it suitable for studying wave phenomena. To capture the dynamics of pulse propagation, we monitored the pulse's evolution at specific coordinates given by $[L/2 + \delta_k, N_0]$. Here, N_0 denotes a fixed position along the N-direction. The parameter δ_k varies within the range $[-80, 80]$ in

increments of 20 sites, allowing us to explore the effects of different spatial offsets on pulse behavior. We then calculated the spectral function $F(\omega)$, defined as $F(\omega) = \frac{1}{M_k}\sum_k f(\omega)_k$, where $f(\omega)_k$ represents the Fourier transform of the wave pulse at the specified position $[L/2+\delta_k, N_0]$ and M_k indicates the number of δ_k values utilized. Specifically, the calculation of $f(\omega)_k$ was performed numerically using the Fast Fourier Transform (FFT) procedure on a long time series of the wave at position $[L/2+\delta_k, N_0]$; we considered approximately 2^{15} points in this time series. This spectral analysis provides insights into the frequency components of the propagating wave, enabling us to understand how different frequencies contribute to the overall pulse dynamics. For our numerical experiments, we set the parameters $L = 240$, $N = 2800$, and $N_0 = 1800$. These values allow for a comprehensive study of pulse behavior across a large lattice, capturing a diverse range of interactions and propagation phenomena. We also considered larger systems; however, within the limits of our computational resources, these system sizes were the largest where we could maintain accurate numerical integration. Additionally, we compute the function Φ, defined as:

$$\Phi = \sum_{i=1}^{L}\sum_{j=N_0}^{N} |\psi_{i,j}(t \to t_{\max})|, \tag{13}$$

with $t_{\max} \approx 1800$ time units. This function serves as an indication of wave propagation, quantifying the total amount of wave packet that successfully traverses the critical point N_0 as time approaches its maximum value. A key observation is that the absence of the wave on the right side of the lattice indicates that propagation did not occur, while the presence of the wave suggests propagation. Therefore, as Φ increases, it provides evidence of wave propagation through the lattice. By summing over all relevant lattice sites, Φ provides a good indication of whether propagation occurs or not, with its growth serving as a sign of successful wave transmission. We will use this, in parallel with spectral analysis, to detect the influence of correlation and other parameters on wave propagation. Through these investigations, we aim to gain an understanding of pulse propagation in media with Lorentzian-correlated disorder.

We emphasize that to start the time integration, the displacement at $t = 0$ is given by the initial condition (i.e., Eq. 12 at $t = 0$), while the displacement prior to $t = 0$ is set to zero, representing a state of rest. This enables the first update using the central-difference scheme. Subsequent time steps proceed without difficulty, as displacements at previous time levels are known. The maximum simulation time, $t_{\max} = 1800$, was chosen for two reasons: first, it is sufficiently long for the wave to propagate far from the initial excitation point (the left boundary); second, it is chosen to ensure the wave does not reach the right boundary of the sample, thus avoiding any undesired reflections.

3. Results

Before presenting our physical quantities, we first provide 3D visualizations of the wave $\psi_{i,j}$ using the $i \times j \times \psi_{i,j}$ coordinates for a qualitative understanding

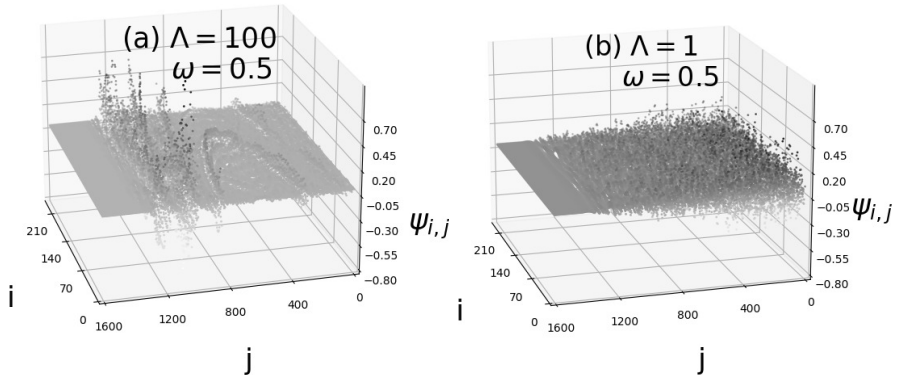

Figure 1: 3D visualization of the wave $\psi_{i,j}$ in the $i \times j \times \psi_{i,j}$ space, for an incident pulse with frequency $\omega = 0.5$ and correlation lengths $\Lambda = 100$ and $\Lambda = 1$.

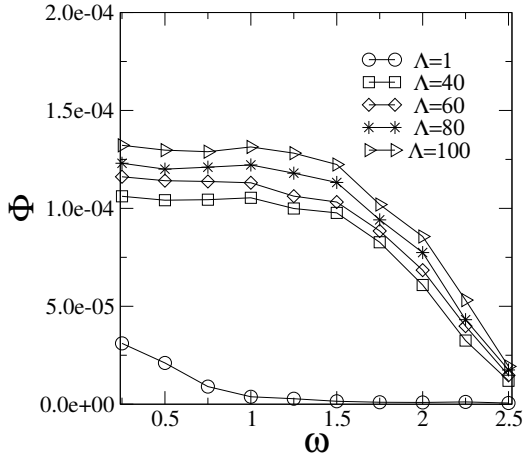

Figure 2: The analysis of the function Φ shows that low-frequency pulses propagate efficiently through highly correlated media ($\Lambda \gg 1$) with minimal energy loss. In contrast, in weakly correlated media ($\Lambda \approx 1$), high-frequency pulses experience significant energy dissipation and distortion due to multiple reflections.

of the system's behavior. We consider an incident pulse with frequency $\omega = 0.5$ and correlation lengths $\Lambda = 100$ and $\Lambda = 1$. The corresponding results are shown in Figure 1. The calculations were performed on a 240×2800 lattice, considering 1200 time units purely for illustration purposes. The visualizations reveal clear differences in wave propagation depending on the correlation length. When $\Lambda = 100$, the pulse, initially inserted at $j = 0$, propagates through a significant portion of the system, indicating enhanced transport. However, due to the presence of disorder—even with strong correlations—some internal scattering occurs, leading to a gradual deformation of the initial pulse. Additionally, the lateral boundaries introduce further perturbations in the propagation along

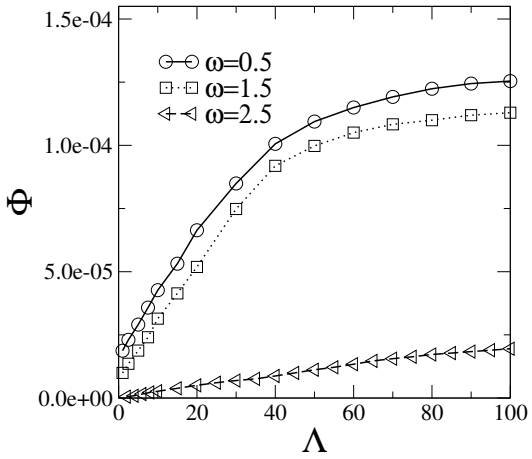

Figure 3: The function Φ versus Λ is shown for $\omega = 0.5, 1.5, 2.5$. For low frequencies ($\omega = 0.5$ and 1.5), the function Φ increases with strong correlations ($\Lambda \gg 1$), while for higher frequencies ($\omega = 2.5$), even in highly correlated systems, Φ remains low, indicating poor transport.

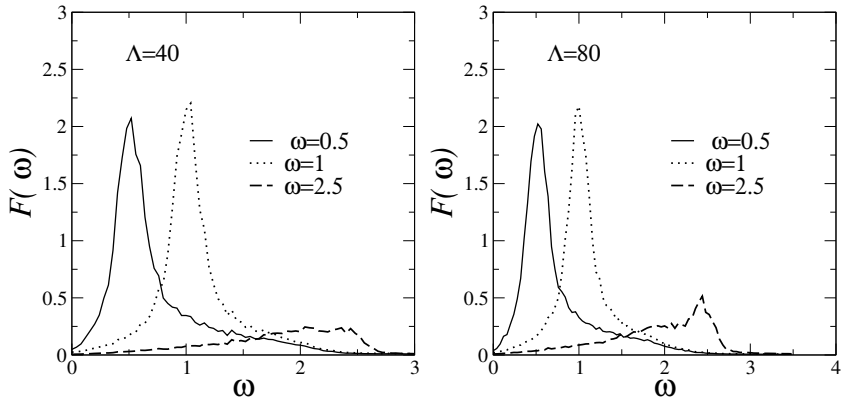

Figure 4: Spectral analysis using the function $F(\omega)$ confirms that low-frequency modes propagate efficiently with minimal distortion, while higher-frequency modes are broadened and attenuated. These findings correlate well with the earlier observations from the function Φ.

the j-direction, influencing the wave's overall shape. Despite these effects, a substantial fraction of the pulse successfully traverses the system. In contrast, for $\Lambda = 1$, the pulse exhibits a very different behavior: a significant portion remains localized near the initial position, suggesting minimal propagation. This highlights the role of correlation length in facilitating wave transport. These visualizations are primarily illustrative, providing an initial qualitative assessment. A more interesting analysis of wave propagation, or lack thereof, will be conducted through measurements of Φ, wave velocity and spectral analysis.

We begin by presenting the main results, starting with the analysis of Figure 2, which illustrates the behavior of the function Φ (see Eq. 13) as a function

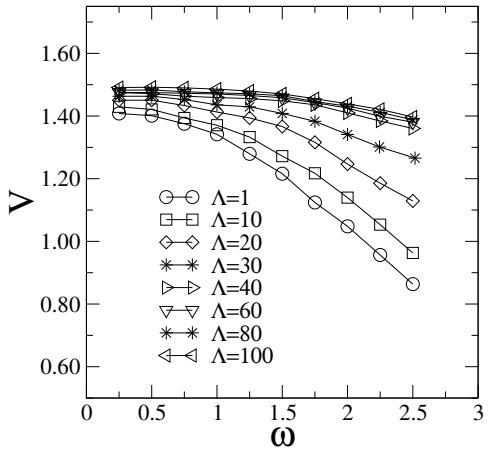

Figure 5: We present the average velocity of the pulse as it propagates to a specific position N_0, calculated as $V = \frac{N_0}{t_0}$ (in units of $\sqrt{\langle \Pi_{i,j} \rangle}$), where t_0 is the time required for the wave's amplitude to exceed a threshold of 10^{-10}. The results show that lower frequencies generally correspond to higher velocities, while higher frequencies lead to a reduction in velocity, particularly in weakly correlated systems ($\Lambda \approx 1$). In contrast, highly correlated systems ($\Lambda \gg 1$) exhibit a weaker frequency-velocity dependence at low frequencies but a more rapid decrease in velocity at higher frequencies, indicating that correlation strength significantly influences wave propagation dynamics.

of the frequency ω. In this study, we considered the incidence of pulses with frequencies ranging from 0.25 to 2.5, covering a wide spectrum of values, and examined how these pulses propagate in media with varying levels of correlation, parametrized by Λ, ranging from 1 to 100. When examining the propagation for low frequencies, such as 0.25 and 0.5, we observe a remarkable behavior of the function Φ, especially when Λ takes on large values ($\Lambda \gg 1$). In this region of strong correlations, Φ remains significantly high, indicating that the pulse propagation is efficient. In other words, there is little energy dissipation as the pulse travels through the medium, even over long distances within the sample. This behavior highlights the crucial role that correlations play in preserving rougly the structure of the shear pulses. As we decrease the value of Λ, approaching $\Lambda = 1$, the scenario changes significantly. For this minimal correlation value, only the pulses with very low frequencies, such as 0.25 and 0.5, manage to propagate reasonably well to regions near the end of the sample. However, even in these cases, the propagation is limited, suggesting that in media with weak correlations, the dispersion and reflection of the pulses increase substantially, hindering wave transmission. At the other extreme, when considering higher frequencies, such as 2.0 and 2.5, the behavior of the function Φ changes drastically, especially for $\Lambda = 1$. In this low correlation scenario, the pulses manage to reach the final region of the sample, but with significantly reduced intensity. The function Φ shows low values, indicating that most of the pulse's energy is dissipated during propagation. Moreover, the shape of the pulse arriving

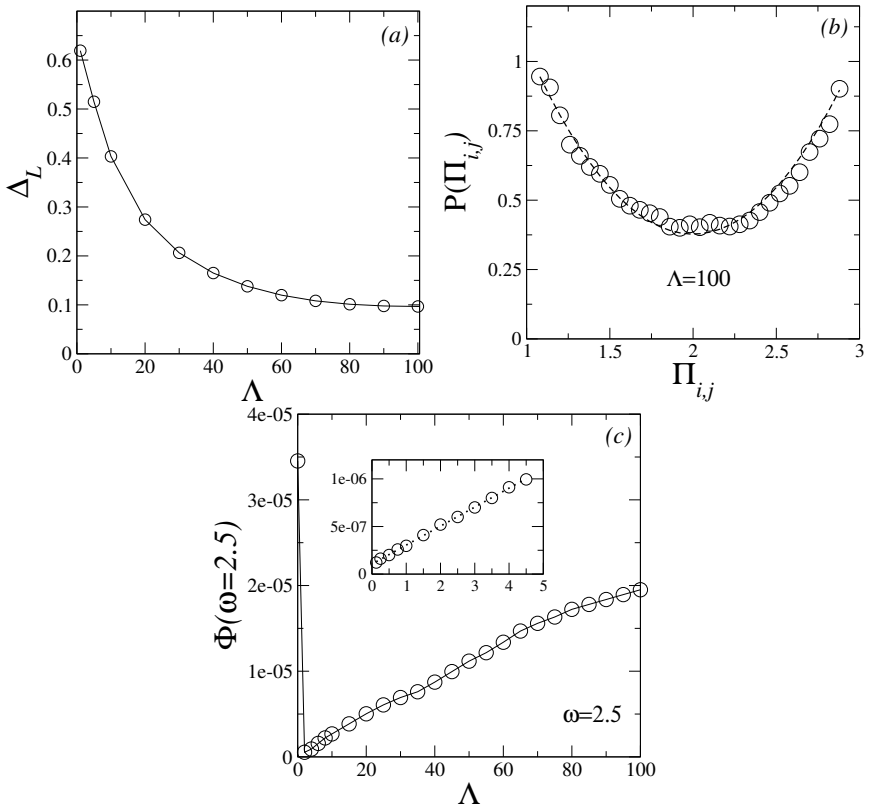

Figure 6: Figure (a) shows how local disorder decreases as the correlation length Λ increases. Figure (b) shows the probability distribution $P(\Pi_{i,j}) \times \Pi_{i,j}$ for $\Lambda = 100$. In Figure (c), the propagation function $\Phi(\omega = 2.5)$ is plotted as a function of Λ, now including the uncorrelated case. We emphasize that in this figure, we place the results for the uncorrelated case at $\Lambda = 0$ for comparison; however, there is no connection to the non-existent limit of $\Lambda = 0$ in Eq. 11. In the inset of Figure (b), we can observe that Φ decreases linearly with Λ.

at the end of the sample is severely distorted. This distortion arises from the multiple reflections and dispersions the pulse encounters as it travels through the disordered medium. This phenomenon is direct evidence of the effect that disorder and lack of correlation have on the propagation of waves, especially at high frequencies. The higher the frequencies, the more severe the effects of multiple reflections, resulting in pulses that are highly deformed, reaching the end of the sample with an unrecognizable shape and a very low amplitude. We will present another figure (fig. 3) that shows the behavior of the function Φ as a function of the localization length Λ for three different frequencies: $\omega = 0.5$, $\omega = 1.5$, and $\omega = 2.5$. For the lower frequencies, $\omega = 0.5$ and $\omega = 1.5$, the function Φ becomes significantly more intense as the correlation strength increases, particularly when $\Lambda \gg 1$. This indicates that for low-frequency modes, strong correlations in the system enhance wave propagation, leading to greater

wave spreading throughout the medium. Essentially, as Λ grows, the system's disorder becomes more correlated over long ranges, allowing the waves to maintain their coherence and energy over larger distances, which is reflected in the larger values of Φ. Another observation from this figure is that the function Φ exhibits two distinct behaviors depending on the value of Λ. For $\Lambda < 40$, Φ grows significantly as Λ increases, indicating that stronger correlations enhance wave propagation. However, for $\Lambda \geq 40$, the growth rate of Φ decreases considerably, suggesting a tendency toward saturation (or near saturation). This behavior indicates that $\Lambda = 40$ appears to act as a threshold where correlations effectively enhance propagation in the system. That is, for $\Lambda < 40$, propagation is not as intense, whereas for $\Lambda > 40$, the system seems to exhibit a more pronounced propagation effect. Beyond this point, further increases in Λ lead to only small improvements in Φ, suggesting a possible limit to the influence of strong correlations on transport efficiency. On the other hand, for the higher frequency $\omega = 2.5$, a very different behavior is observed. Even when Λ reaches large values, such as $\Lambda = 100$, the function Φ remains small, indicating low energy transport across the system. This suggests that for high-frequency modes, strong correlations in the medium are not sufficient to sustain efficient propagation. Instead, the higher frequency pulses undergo significant scattering and attenuation, leading to poor transmission. This behavior aligns with previous observations that higher frequency waves are more susceptible to multiple reflections and dispersion within disordered systems, even when the disorder is strongly correlated. In summary, while strong correlations ($\Lambda \gg 1$) greatly enhance the propagation of low-frequency modes, they do not have the same effect on high-frequency modes, as evidenced by the consistently low values of Φ for $\omega = 2.5$. This highlights a frequency-dependent behavior in wave transport, where low-frequency waves benefit from the system's correlations, whereas high-frequency waves do not propagate as effectively, even under the same conditions of strong correlation.

Now, we will present the spectral analysis through the function $F(\omega)$ (see fig. 4). We will showcase various calculations for $\Lambda = 40$ and $\Lambda = 80$. The results clearly indicate that, in the low-frequency region, $F(\omega)$ exhibits well-defined peaks at frequencies that precisely match the input frequencies applied at the left boundary of the system. This strongly suggests the existence of propagation across the sample with minimal destruction or dispersion of the wave packet. In this low-frequency region, it is also worth noting that the function Φ demonstrated significantly high values, reinforcing this observation. The combination of these findings — well-defined spectral peaks and high values of the function Φ — provides strong evidence for the efficient propagation of low-frequency modes throughout the system. On the other hand, for higher frequencies, such as $\omega = 2.5$, we observe a broadened spectral function with considerably lower intensity. This is in good agreement with the reduction in propagation efficiency, as already demonstrated by the function Φ in the previous figure. The broadening of the spectral peaks and the decrease in intensity at higher frequencies indicate that the wave packet undergoes significant distortion and attenuation as it travels through the disordered medium, leading

to reduced propagation in this regime. In summary, the spectral analysis confirms the earlier observations, highlighting a clear correlation between frequency and wave propagation efficiency in the system. Low-frequency modes propagate more efficiently with less distortion, while high-frequency modes are significantly attenuated and broadened, aligning with the diminished propagation observed in the function Φ.

In fig. 5 we present the results regarding the average velocity of the pulse as it travels from the left side of the sample to a specific position N_0. The velocity, in this context, will be calculated as $V = \frac{N_0}{t_0}$, where t_0 represents the time required for the modulus of the wave at position N_0 to exceed a threshold of 10^{-10}. This criterion ensures that we are tracking when the pulse reaches a detectable amplitude at N_0. It is worth emphasizing that, since the characteristic time scale is proportional to $1/\sqrt{\langle \Pi \rangle}$, the ratio N_0/t_0 has units proportional to $\sqrt{\langle \Pi_{i,j} \rangle}$. The graph reveals interesting behavior concerning the relationship between frequency and velocity. For lower frequencies, the velocity of the pulse tends to be slightly higher compared to that of higher frequencies. This indicates that, as the frequency increases, there is a small but noticeable reduction in the velocity of the wave as it propagates through the medium. However, the magnitude of this frequency-dependent behavior varies depending on the correlation strength within the system. In highly correlated systems, where $\Lambda \gg 1$, the frequency-velocity dependence is relatively weak for $\omega \leq 1.5$, with the velocity remaining nearly constant across this frequency range. This suggests that strong correlations in the medium help maintain the wave's speed. However, for $\omega > 1.5$, the velocity starts to decrease more rapidly as the frequency increases, indicating a slightly stronger influence of frequency on wave propagation in this higher frequency regime, even in the presence of strong correlations. On the other hand, in systems with weaker correlations (Λ close to 1), the relationship between velocity and frequency becomes much more pronounced. In these cases, the velocity decreases more significantly as the frequency increases, implying that weaker correlations lead to more substantial interactions between the pulse and the disordered medium, which in turn affects the wave's ability to maintain its speed. This strong frequency dependence in less correlated systems highlights the role of disorder in influencing the propagation dynamics of waves. In summary, while the velocity of the pulses shows only slight frequency dependence in highly correlated media, it exhibits a much stronger dependence in weakly correlated systems, where the disorder in the medium has a more significant impact on wave propagation. We would like to emphasize that our results were not very satisfactory for $\omega > 2.5$. Within the system sizes we considered and the times we were able to integrate with reasonable accuracy, the wave packet did not propagate macroscopically to positions near the end of the lattice, and the velocity calculations were unsuccessful. Therefore, significantly increasing either the simulation time or the system size (for example, to avoid boundary effects along the L direction) was not feasible within our computational limitations. We believe that the wave packet should still propagate slowly at frequencies slightly higher than $\omega = 2.5$, but, for now, we were unable

to conduct an analysis at much higher frequencies. We regret this limitation.

Before concluding our work, we will analyze the propagation of high frequencies, focusing on $\omega = 2.5$ as an example, and compare this propagation at the same frequency in systems without correlations. We will examine the behavior of Φ in systems with strong correlations (i.e., $\Lambda \approx 100$) and compare these results with those obtained in systems without correlations (i.e., with uncorrelated disorder). To do this, we will generate samples with uncorrelated disorder, ensuring that their statistical properties are similar to those of the correlated case, particularly in situations with strong correlations. In summary, we will compare the propagation of high-frequency shear waves in a correlated system with the same propagation at high frequencies in a system that has uncorrelated disorder, which exhibits statistical properties similar to those of the correlated disorder. One of the interesting statistical properties that can classify a disorder distribution is the local disorder Δ_L. Local disorder is calculated by dividing a sample of size $L \times N$ into u boxes of size $d_0 \times d_0 = 40 \times 40$, and computing $\sigma_u = \sqrt{\langle \Pi_{i,j}^2 \rangle_u - \langle \Pi_{i,j} \rangle_u^2}$, where

$$\langle \Pi_{i,j}^2 \rangle_u = \frac{1}{A_u} \sum_{\langle i,j \rangle_u} \Pi_{i,j}^2 \quad \text{and} \quad \langle \Pi_{i,j} \rangle_u = \frac{1}{A_u} \sum_{\langle i,j \rangle_u} \Pi_{i,j}, \tag{14}$$

with $A_u = d^2$ representing the number of sites within each box u, and $\langle i, j \rangle_u$ denoting a sum over the sites i, j within the box u. The local disorder is then defined as $\Delta_L = \frac{1}{N_u} \sum_u \sigma_u$, where N_u is the total number of boxes. It is important to emphasize that as Λ increases, the local disorder Δ_L decreases (see results in Fig. 6(a) for reference). We can see that for $\Lambda \approx 1$, the local disorder is close to 0.61, while for $\Lambda = 100$, the local disorder is approximately 0.1. Therefore, since we wish to compare the propagation in the high-frequency region in strongly correlated systems and in uncorrelated systems, we need to generate uncorrelated samples with $\Delta_L \approx 0.1$. Another relevant statistical point is to respect the probability distribution for elasticity. Therefore, we need to generate uncorrelated samples where the probability distribution exhibits the same behavior as that found in the case with $\Lambda = 100$. In practical terms, we measure the normalized distribution $P(\Pi_{i,j}) \times \Pi_{i,j}$ for $\Lambda = 100$ (see Fig. 6(b)). The best fit (dashed line) yields the following parabolic equation: $P(\Pi_{i,j}) \approx a_0 + a_1(\Pi_{i,j} - 2)^2$ with $a_0 \approx 0.37$ and $a_1 \approx 0.68$. We then use this distribution to generate uncorrelated samples, ensuring that the uncorrelated system we consider follows the same probability distribution. Additionally, we normalize the uncorrelated disorder distribution to maintain the same local disorder as in the correlated profile with $\Lambda = 100$. Specifically, we set the uncorrelated disorder to have an average of 2 and the local disorder approximately 0.1. In Fig. 6(c), we compare $\Phi(\omega = 2.5)$ as a function of Λ with $\Phi(\alpha = 2.5)$ for the previously defined uncorrelated disorder. Here, the data for the uncorrelated case is included at $\Lambda = 0$. We emphasize that this point at $\Lambda = 0$ is presented solely for comparison with the other results—there is no physical connection between this data point at $\Lambda = 0$ and the irrelevant limit $\Lambda = 0$ in Eq. 11. Our results show that, when considering an incident pulse with high frequency ($\omega = 2.5$), the uncorrelated

case ($\Lambda = 0$) exhibits more wave propagation than strongly correlated cases. In other words, this correlation model, even in the strong correlation limit, is more opaque to the transport of vibrational modes than an uncorrelated system with the same local disorder magnitude—though this effect is observed only in the high-frequency regime (i.e., for small wavelengths). In the works by Izrailev and co-workers (see Ref.[27] for an instructive review), it is shown, within the context of the Anderson model, that in high-energy regions (i.e., for small wavelengths), localization becomes stronger in systems with correlated disorder compared to those with uncorrelated disorder. They explain this phenomenon by noting that the presence of correlations in the disorder distribution creates more effective barriers for wave propagation, leading to enhanced localization. Our results suggest that, within the type of correlated disorder we are using and the lattice vibration framework we are considering, this phenomenon also occurs.

4. Summary

This paper investigates shear wave propagation through disordered media with varying levels of correlation, focusing on the analysis of the function Φ, spectral behavior, and pulse velocity as functions of both frequency and correlation length (Λ). The results show that at low frequencies and strong correlations ($\Lambda \gg 1$), wave propagation becomes more efficient. In this regime, a significant portion of the wave packet propagates over long distances, as indicated by the increase in the function Φ, the higher velocity, and well-defined spectral peaks. These characteristics suggest that the medium's strong correlations play a crucial role in facilitating more coherent wave transport. The correlations help preserve the wave packet profile, reducing scattering and reflection, which are typically observed in disordered systems. As the correlation length increases, the system exhibits more robust wave propagation, with a higher degree of coherence and less dispersion, allowing the wave to maintain its shape over longer distances. This behavior contrasts with cases of weak correlations ($\Lambda \ll 1$), where scattering dominates, leading to slower propagation of the wave packet.

Conversely, at higher frequencies ($\omega \geq 2.0$), even under conditions of strong correlation ($\Lambda \gg 1$), wave propagation is less efficient. In our calculations for higher frequencies the function Φ remains small, indicating poor wave transmission, while the spectral peaks become broadened and less intense, suggesting a loss of coherence and significant pulse distortion. In weakly correlated systems ($\Lambda \approx 1$), the situation is even more pronounced, with both low and high-frequency waves exhibiting limited propagation. Here, disorder dominates, leading to increased wave dispersion, reduced pulse velocity, and highly distorted waveforms at the end of the sample. The velocity analysis further supports these findings, showing a clear reduction in pulse speed with increasing frequency, particularly in weakly correlated media. These results highlight a frequency-dependent transport mechanism in disordered systems, where low-frequency modes benefit significantly from strong correlations, while high-frequency modes are heavily impeded by scattering effects. This behavior underscores the importance of correlation length Λ in controlling the transport

properties of the system. We emphasize that high-frequency modes (i.e., modes with shorter wavelengths) are generally more susceptible to Anderson localization and disorder effects.[27] This is because shorter wavelengths are more sensitive to the spatial irregularities and inhomogeneities in the system, leading to stronger scattering and localization. As a result, high-frequency modes tend to become more localized, especially in disordered systems, where their propagation is hindered by the disorder present in the medium. This behavior has been increasingly demonstrated in the context of the Anderson electronic model, where higher-frequency excitations are shown to exhibit stronger localization due to disorder .[27] Our results for the propagation of high-frequency shear waves in two-dimensional systems with Lorentzian-correlated disorder are consistent with those originally observed in the Anderson model. Furthermore, the study suggests a near-saturation effect in wave transport efficiency at very large Λ values (e.g., $\Lambda \geq 40$), where further increases in correlation strength lead to diminishing returns. For $\Lambda > 40$, both the function Φ and the velocity become nearly constant, with only small increases observed. This behavior indicates that, beyond a certain threshold, the influence of correlation strength on wave propagation diminishes, and the system enters a regime where transport is only slightly affected by further increases in Λ. Although there is a small increase in the transport indicators, this increase is no longer as pronounced. As a result, wave transport efficiency roughly stabilizes, suggesting that the correlation effects reach their maximum impact at these Λ values.

Looking ahead, this research offers valuable insights into the design of engineered materials with specific wave propagation properties. By carefully tuning correlation strength, it is possible to enhance or suppress wave transmission for targeted frequency ranges. This has practical applications in fields such as insulation, wave-based information transfer, and the development of metamaterials for manipulating sound waves in novel ways. Moreover, the study provides a foundation for exploring more complex scenarios, such as nonlinear disordered media, time-dependent correlations, or systems with a broader range of frequencies. These extensions could lead to new technologies in controlling wave propagation across a variety of disciplines, from telecommunications to medical ultrasound imaging.

5. Acknowledgments

This work was partially supported by CNPq, CAPES, and FINEP (Federal Brazilian Agencies), as well as FAPEAL (Alagoas State Agency).

References

[1] J. R. Tempelman, T. Weidemann, E. B. Flynn, K. H. Matlack, A. F. Vakakis, Physics-informed machine learning for the inverse design of wave scattering clusters, Wave Motion 130 (2024) 103371.

[2] D. Churochkin, F. Lund, Diffusion of elastic waves in a two dimensional continuum with a random distribution of screw dislocations, Wave Motion 69 (2017) 16–34.

[3] M. Akaberian, S. Jafari, M. R. Rahimi Tabar, K. Esfarjani, Delocalization of phonons and energy spectrum in disordered nonlinear systems, Phys. Rev. B 101 (2020) 220301.

[4] D. M. Photiadis, Theory of vibration propagation in disordered media, Wave Motion 45 (1) (2007) 30–47, special Issue on Localization of Wave Motion.

[5] H. Hamzehpour, M. Asgari, M. Sahimi, Acoustic wave propagation in heterogeneous two-dimensional fractured porous media, Phys. Rev. E 93 (2016) 063305.

[6] M. Franco, E. Calzetta, Wave propagation in non-gaussian random media, Journal of Physics A: Mathematical and Theoretical 48 (4) (2015) 045206.

[7] Z.-Z. Yan, C. Zhang, Y.-S. Wang, Wave propagation and localization in randomly disordered layered composites with local resonances, Wave Motion 47 (7) (2010) 409–420.

[8] H. Hamzehpour, F. H. Kasani, M. Sahimi, R. Sepehrinia, Wave propagation in disordered fractured porous media, Phys. Rev. E 89 (2014) 023301.

[9] B. Kramer, A. MacKinnon, Localization: theory and experiment, Reports on Progress in Physics 56 (12) (1993) 1469.

[10] M. P. S. Júnior, M. L. Lyra, F. A. B. F. de Moura, Delocalized vibrational modes in disordered harmonic chains with correlated spring constants, Acta Phys. Pol. B 46 (2016) 1247.

[11] C. A. A. dos Santos, T. F. Assunção, M. L. Lyra, F. A. B. F. de Moura, Energy dynamics in a one-dimensional aperiodic anharmonic lattice, International Journal of Modern Physics C 23 (08) (2012) 1240009.

[12] H. Afsar, G. Peiwei, M. Aldandani, Y. Akbar, M. M. Alam, Analyzing the acoustic wave propagation characteristics in discontinuous bifurcated waveguide, Chaos, Solitons & Fractals 172 (2023) 113499.

[13] A. Bouchendouka, Z. E. A. Fellah, C. T. Nguyen, E. Ogam, C. Perrot, A. Duval, C. Depollier, Improving acoustic wave propagation models in highly attenuating porous materials, The Journal of the Acoustical Society of America 155 (1) (2024) 206–217.

[14] Y. Fan, X. Ji, X. Liu, P. Cai, The nonlinear analysis of elastic wave of piezoelectric crystal plate with perturbation method, Wave Motion 51 (5) (2014) 798–803.

[15] A. I. Adham, V. Sorokin, B. Mace, A. Hall, Broadband vibration isolation in a finite elastic rod with tailored resonators, Wave Motion 136 (2025) 103528.

[16] R. Sepehrinia, A. Bahraminasab, M. Sahimi, M. R. R. Tabar, Dynamic renormalization group analysis of propagation of elastic waves in two-dimensional heterogeneous media, Phys. Rev. B 77 (2008) 014203.

[17] P. W. Anderson, Absence of diffusion in certain random lattices, Physical Review 109 (5) (1958) 1492–1505.

[18] S. E. Skipetrov, S. Pilati, Anderson localization of sound in three dimensions, Physical Review Letters 112 (2) (2014) 023905.

[19] A. Ghosh, S. Sengupta, Manipulating sound transmission with geometric disorder in elastic networks, Physical Review Letters 119 (8) (2017) 084301.

[20] A. Z. Genack, A. D. Stone, Introduction to Wave Transport in Random Media: From Single Photonics to Sound, Cambridge University Press, 2018.

[21] Y. Li, J. H. Page, Wave Propagation in Random and Complex Media: Theory and Applications, CRC Press, 2019.

[22] P. Sebbah, Waves and Imaging through Complex Media, Kluwer Academic Publishers, 2002.

[23] M. Fink, Time-reversed acoustics, Scientific American 280 (2) (1999) 94–99.

[24] F. Shahbazi, A. Bahraminasab, S. M. Vaez Allaei, M. Sahimi, M. R. R. Tabar, Localization of elastic waves in heterogeneous media with off-diagonal disorder and long-range correlations, Phys. Rev. Lett. 94 (2005) 165505.

[25] A. E. B. Costa, F. A. B. F. de Moura, Localization of acoustic waves in one-dimensional models with chaotic elasticity, International Journal of Modern Physics C 22 (06) (2011) 573–580.

[26] S. M. V. Allaei, M. Sahimi, M. R. R. Tabar, Propagation of acoustic waves as a probe for distinguishing heterogeneous media with short-range and long-range correlations, Journal of Statistical Mechanics: Theory and Experiment 2008 (03) (2008) P03016.

[27] F. Izrailev, A. Krokhin, N. Makarov, Anomalous localization in low-dimensional systems with correlated disorder, Physics Reports 512 (3) (2012) 125–254, anomalous localization in low-dimensional systems with correlated disorder.

[28] P. M. Morse, K. U. Ingard, Theoretical acoustics (1968).

[29] K. R. Symon, Mechanics, 2nd Edition, Addison-Wesley, Reading, MA, 1960.

[30] L. D. da Silva, A. R. Neto, M. O. Sales, J. L. L. dos Santos, F. A. B. F. de Moura, Propagation of vibrational modes in classical harmonic lattice with correlated disorder., Annals of the Brazilian Academy of Sciences 91 (2019) e20180114.

[31] K. M. Abualnaja, Finite difference method for solving a physical problem in fluid flow, International Journal of Modern Physics C 32 (02) (2021) 2150025.

[32] L. D. da Silva, J. L. L. dos Santos, A. R. Neto, M. O. Sales, , F. A. B. F. de Moura, One-electron propagation in fermi, pasta, ulam disordered chains with gaussian acoustic pulse pumping, International Journal of Modern Physics C 28 (08) (2017) 1750100.

[33] J. Strikwerda, Finite Difference Schemes and Partial Differential Equations, 2nd Edition, SIAM, Philadelphia, PA, 2004.

[34] T. J. R. Hughes, The Finite Element Method: Linear Static and Dynamic Finite Element Analysis, Dover, New York, 2000.

[35] R. E. Mickens, Nonstandard finite difference schemes for differential equations, Journal of Difference Equations and Applications 8 (2002) 823–847.

[36] M. Joaquim, S. Scheer, Finite-difference time-domain method for three-dimensional grid of hexagonal prisms, Wave Motion 63 (2016) 32–54.

[37] J. Rashidinia, M. N. Rasoulizadeh, Numerical methods based on radial basis function-generated finite difference (rbf-fd) for solution of gkdvb equation, Wave Motion 90 (2019) 152–167.

[38] W. Desmet, D. Vandepitte, Finite Element Method for Acoustics, Katholieke Universiteit Leuven, 2008.